

# Acridinium Salt-Based Fluoride and Acetate Chromofluorescent Probes: Molecular Insights into Anion Selectivity Switching

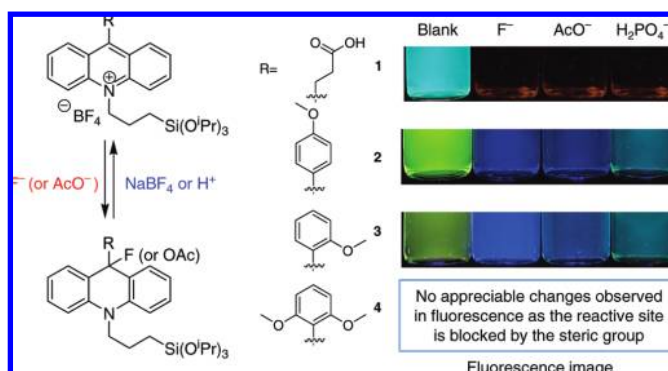
Yu-Chen Lin and Chao-Tsen Chen\*

Department of Chemistry, National Taiwan University, Taipei, Taiwan 106, ROC

chenct@ntu.edu.tw

Received August 20, 2009

## ABSTRACT



A series of acridinium salt-based probes capable of detecting fluoride and acetate anions via a nucleophilic attack at the C9 position of the acridinium moiety is reported. The formation of corresponding acridane displays drastic changes, in both UV–vis absorption and fluorescence emission. The sensing mechanism is a reversible process upon treating either tetrafluoroborate salt or an acid.

Anions are commonly found in the environment and biological systems. For instance, fluoride is widely used in dental care applications and exhibits inhibition of certain enzyme functions.<sup>1</sup> In addition to playing a central role in biological regulation, chloride is also a major groundwater contaminant that can corrode steel and concrete.<sup>2</sup> Thyroid hormone synthesis largely determines iodine content.<sup>3</sup> Acetate is a possible tracer for malignancies and has been extensively investigated in prostate cancer and its metastases.<sup>4</sup> Phosphate ion is biologically and environmentally significant.<sup>5</sup> Cyanide

exerts adverse effects on human health as well as environment at low concentrations. Determining anions concentration is thus of primary concern in many areas, including food processing, industry, and clinic analysis.<sup>6</sup> However, hydrophilic anions, such as  $F^-$  and  $Cl^-$ , form strong hydrogen bonds with protic solvents. Therefore, developing fluorescent probes based on electrostatic interactions for anions functioning in polar protic solvents is both challenging and currently infeasible.<sup>7</sup>

Currently, analytes that form covalent bonds with receptors to trigger highly selective reactions and induce changes in

(1) (a) Săndulescu, R.; Florean, E.; Roman, L.; Mirel, S.; Oprean, R.; Suciu, P. *J. Pharm. Biomed. Anal.* **1996**, *14*, 951–958. (b) Michigami, Y.; Kuroda, Y.; Ueda, K.; Yamamoto, Y. *Anal. Chim. Acta* **1993**, *274*, 299–302.

(2) (a) Sonawane, N. D.; Thiagarajah, J. R.; Verkman, A. S. *J. Biol. Chem.* **2002**, *277*, 5506–5513. (b) Thangavel, K.; Rengaswamy, N. S. *Cem. Concr. Compos.* **1998**, *20*, 283–292.

(3) Burguera, J. L.; Brunetto, M. R.; Contreras, Y.; Burguera, M.; Gallignani, M.; Carrero, P. *Talanta* **1996**, *43*, 839–850.

(4) (a) Kuhajda, F. P.; Pizer, E. S.; Li, J. N.; Mani, N. S.; Frehywot, G. L.; Townsend, C. A. *Proc. Natl. Acad. Sci. U.S.A.* **2000**, *97*, 3450–3454. (b) Văvere, A. L.; Kridel, S. J.; Wheeler, F. B.; Lewis, J. S. *J. Nucl. Med.* **2008**, *49*, 327–334.

(5) (a) Beer, P. D. *Acc. Chem. Res.* **1998**, *31*, 71–80. (f) Miyaji, H.; Sessler, J. L. *Angew. Chem., Int. Ed.* **2001**, *40*, 154–157.

(6) Geddes, C. D. *Meas. Sci. Technol.* **2001**, *12*, R53–R88.

fluorescence emission or absorption are being used to design target-specific chromogenic/fluorogenic probes.<sup>8</sup> Nucleophilic  $\text{CN}^-$  opening of the oxazine ring inducing a dramatic color change was studied to determine cyanide levels.<sup>9</sup> Reactive groups, such as trifluoroacetyl<sup>10</sup> and the formyl<sup>11</sup> moiety capable of reacting with nucleophiles, have been applied to either cyanide or hydrogen sulfite detection. Additionally, the transformation of pyrilium to thiopyrilium salt was examined to develop a selective probe for the sulfide anion.<sup>12</sup> Moreover, the strong interaction of boron–fluoride<sup>13</sup> or silicon–fluoride<sup>14</sup> was studied to develop fluoride molecular sensors. A recent study examined the feasibility of using  $\text{OCl}^-$  to selectively oxidize the hydrazo group into diimide.<sup>15</sup>

A nucleophilic attack occurs at the highly electron-deficient C9 position of acridinium salts more readily than at the corresponding position in their pyridinium or quinolinium counterparts.<sup>16</sup> This reactivity has been exploited to develop several functional materials.<sup>17,18</sup> For instance, a photoreversible molecular machine with a bulky 9-alkoxy acridane moiety undergoes photoheterolysis to form an acridinium with a planar geometry.<sup>17</sup> Herein, we examine the feasibility of using this reaction feature to develop acridinium-based chromogenic and fluorescent sensors **1–4** (Figure 1) for anion detection. In addition to playing a role in anion recognition, the acridinium moiety also functions as a signaling unit. The recognition is based mainly on nucleophilic addition and the dearomatization of the acridinium moiety after the addition gives rise to the drastic changes in UV–vis absorption and fluorescence emission characteristics serving as signal outputs.

Probe **1** and acridinium derivatives have been used for the determination of  $\text{Cl}^-$ ,  $\text{Br}^-$ , and  $\text{I}^-$  in aqueous media; however, this probe has not been used for the estimation of other anions.<sup>6,19</sup> Thus, we reexamined the anion selectivity profile of probe **1**. During the preparation of **1**, we found a

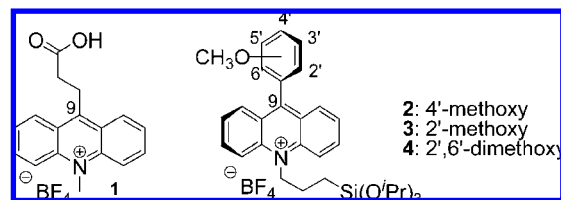
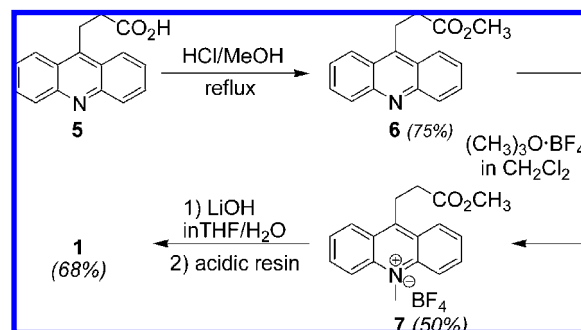


**Figure 1.** Chemical structures of probes **1–4**.

low conversion in *N*-methylation by using either a sealed glass tube or pressure vessels. Additionally, over methylated byproducts and carbon residue were produced. Thus, a new synthetic route was sought (Scheme 1). Esterification of 3-acridin-9-yl propionic acid (**5**)<sup>20</sup> with methanol in the presence of concentrated hydrochloric acid as a catalyst produced a methyl ester (**6**) in 75% yield. Treatment of **6** with trimethyloxonium fluoroborate ( $(\text{CH}_3)_3\text{O}^+\text{BF}_4^-$ )<sup>21</sup> followed by a base-promoted hydrolysis yielded probe **1**.

**Scheme 1.** New Synthetic Route for the Synthesis of Probe **1**



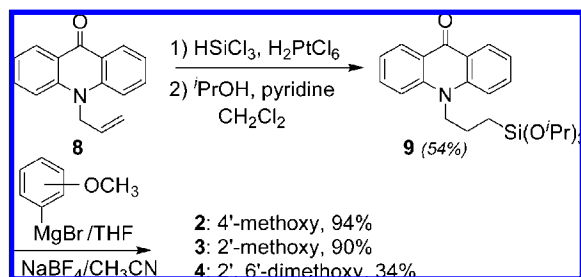
Probes **2–4** were obtained using similar synthetic routes (Scheme 2). By starting with 10-allyl-9(10*H*)-acridone (**8**), platinum-catalyzed hydrosilylation of terminal alkene produced triisopropoxy silane-modified acridone (**9**). Coupling of **9** with a substituted phenyl Grignard reagent followed by counterion exchange yielded various 9-phenyl acridinium derivatives (**2–4**). The bulky triisopropoxy silane group in **9** can prevent the Grignard reagent from undergoing nucleophilic substitution to yield phenyl silane byproducts,<sup>22</sup> as well as being used to further derive solid supports.

Photospectroscopic features of probes **1–4** were characterized by UV–vis absorption and fluorescence emission. Probe **1** exhibited three absorption bands appearing at 261 ( $\epsilon = 64\,900\text{ M}^{-1}\text{ cm}^{-1}$ ), 360 ( $\epsilon = 15\,070\text{ M}^{-1}\text{ cm}^{-1}$ ), and 419 ( $\epsilon = 4060\text{ M}^{-1}\text{ cm}^{-1}$ ) nm, respectively; a blue-green fluorescence appeared at 495 nm in  $\text{CH}_3\text{CN}$ . The longest wave-

- (7) (a) Beer, P. D.; Gale, P. A. *Angew. Chem., Int. Ed.* **2001**, *40*, 486–516. (b) Aydogan, A.; Coady, D. J.; Kim, S. K.; Akar, A.; Bielawski, C. W.; Marquez, M.; Sessler, J. L. *Angew. Chem., Int. Ed.* **2008**, *47*, 9648–9652.
- (8) (a) Ros-Lis, J. V.; Martínez-Mañez, R.; Soto, J. *Chem. Commun.* **2002**, 2248–2249. (b) Yang, Y.-K.; Yook, K.-J.; Tae, J. *J. Am. Chem. Soc.* **2005**, *127*, 16760–16761. (c) Song, F.; Garner, A. L.; Koide, K. *J. Am. Chem. Soc.* **2007**, *129*, 12354–12355. (d) Sun, Z.-N.; Liu, F.-Q.; Chen, Y.; Tam, P. K. H.; Yang, D. *Org. Lett.* **2008**, *10*, 2171–2174. (e) Yang, Y.-K.; Cho, H. J.; Lee, J.; Shin, I.; Tae, J. *Org. Lett.* **2009**, *11*, 859–861. (f) Chatterjee, A.; Santra, M.; Won, N.; Kim, S.; Kim, J. K.; Kim, S. B.; Ahn, K. H. *J. Am. Chem. Soc.* **2009**, *131*, 2040–2041. (g) Garner, A. L.; St Croix, C. M.; Pitt, B. R.; Leikauf, G. D.; Ando, S.; Koide, K. *Nat. Chem.* **2009**, *1*, 1–6.
- (9) Tomasulo, M.; Raymo, F. M. *Org. Lett.* **2005**, *7*, 4633–4636.
- (10) Chung, Y. M.; Raman, B.; Kim, D.-S.; Ahn, K. H. *Chem. Commun.* **2006**, 186–188.
- (11) (a) Mohr, G. *J. Chem. Commun.* **2002**, 2646–2647. (b) Mohr, G. *J. Chem.–Eur. J.* **2004**, *10*, 1082–1090.
- (12) Jimnez, D.; Martínez-Mañez, R.; Sancen, F.; Ros-Lis, J. V.; Benito, A.; Soto, J. *J. Am. Chem. Soc.* **2003**, *125*, 9000–9001.
- (13) (a) Koskela, S. J. M.; Fylesb, T. M.; James, T. D. *Chem. Commun.* **2005**, 945–947. (b) Xu, S.; Chen, K.; Tian, H. *J. Mater. Chem.* **2005**, *15*, 2676–2680. (c) Hudnall, T. W.; Gabbai, F. P. *Chem. Commun.* **2008**, 4596–4597.
- (14) (a) Jiang, X.; Vieweger, M. C.; Bollinger, J. C.; Dragnea, B.; Lee, D. *Org. Lett.* **2007**, *9*, 3579–3582. (b) Kim, S. Y.; Hong, J.-I. *Org. Lett.* **2007**, *9*, 3109–3112.
- (15) Chen, X.; Wang, X.; Wang, S.; Shi, W.; Wang, K.; Ma, H. *Chem.–Eur. J.* **2008**, *14*, 4719–4724.
- (16) Acheson, R. M. *Chemistry of Heterocyclic Compounds*; John Wiley & Sons, Inc.: New York, 1973; Vol. 9, pp 433–517.
- (17) (a) Abraham, W.; Buck, K.; Orda-Zgadaj, M.; Schmidt-Schäffera, S.; Grummt, U.-W. *Chem. Commun.* **2007**, 3094–3096. (b) Grubert, L.; Abraham, W. *Tetrahedron* **2007**, *63*, 10778–10787.
- (18) Yang, Y.-K.; Tae, J. *Org. Lett.* **2006**, *8*, 5721–5723.

- (19) (a) Urbano, E.; Offenbacher, H.; Wolfbeis, O. S. *Anal. Chem.* **1984**, *56*, 427–429. (b) Geddes, C. D. *Dyes Pigm.* **2000**, *45*, 243–251.
- (20) Veveřková, E.; Nosková, M.; Toma, Š. *Synth. Commun.* **2002**, *32*, 729–733.
- (21) Clennan, E. L.; Liao, C.; Ayokosok, E. *J. Am. Chem. Soc.* **2008**, *130*, 7552–7553.
- (22) Lindner, E.; Salesch, T. *J. Organomet. Chem.* **2001**, *628*, 151–154.

**Scheme 2.** Synthesis of Probes 2, 3, and 4



lengths of probes **2**, **3**, and **4** in  $\text{CH}_2\text{Cl}_2$  were red-shifted to 448, 430, and 430 nm, respectively, owing to a charge shift process between the methoxy phenyl ring (electron donor group) and the acridinium salts (Figure S1 in Supporting Information).<sup>23</sup> Probes **2** and **3** displayed a yellow fluorescence around 536 nm, while **2** exhibited a fluorescence intensity 16-fold higher than that of **3**, whereas fluorescence was scarcely visible in **4**.

The fluorescence sensing profiles of probes **1** and **2** for various anions ( $\text{F}^-$ ,  $\text{Cl}^-$ ,  $\text{Br}^-$ ,  $\text{I}^-$ ,  $\text{CN}^-$ ,  $\text{SCN}^-$ ,  $\text{AcO}^-$ ,  $\text{NO}_3^-$ ,  $\text{ClO}_4^-$ ,  $\text{HSO}_4^-$ , and  $\text{H}_2\text{PO}_4^-$  with a tetrabutylammonium counterion) were investigated by high-throughput fluorescence screening in  $\text{CH}_3\text{CN}$  and  $\text{CH}_2\text{Cl}_2$ , respectively. Detailed results can be found in the Supporting Information (Figure S2–S6). Among the 11 anions screened, the halide anions quenched the fluorescence of probes **1** and **2** to a slight extent, and the quenching efficiency increased in the order from  $\text{Cl}^-$  to  $\text{Br}^-$  to  $\text{I}^-$ .<sup>6</sup> Once  $\text{F}^-$ ,  $\text{AcO}^-$ ,  $\text{CN}^-$ , or  $\text{H}_2\text{PO}_4^-$  was added, the fluorescence emission intensity at 495 nm of **1** was quenched completely, whereas probe **2** displayed a fluorescence decrease at 536 nm with a concomitant increase at 415 nm (Figure 2a). The disappearance of the three characteristic absorption peaks corresponding to the acridinium salts and the newly formed peaks at 280 nm for **1** and 288 nm for **2** strongly suggested transformation of the acridinium moiety into the corresponding acridane via anionic addition to the C9 position of the former (Figure 2b).

The addition of  $\text{F}^-/\text{AcO}^-$  to **2** was further confirmed by monitoring the changes in its  $^1\text{H}$  NMR spectra in the presence of either  $\text{F}^-$  or  $\text{AcO}^-$  (Figure 3). Four peaks of acridinium of **2** showed pronounced upfield shifts due to the conversion of acridinium to acridane in 5 equiv of either  $\text{F}^-$  (Figure 3b) or  $\text{AcO}^-$  (Figure 3c). The largest chemical shifts were observed for the proton ( $\Delta H^a = 1.48$  ppm) adjacent to the central pyridinium ring and *para*-protons ( $\Delta H^c = 1.47$  ppm) with respect to the nitrogen of pyridinium. These chemical shifts in the aromatic region of the resulting nucleophilic adduct **2-F** were consistent with the counterparts of 9,10-dihydro-9-methoxy-9-(4-methoxyphenyl)-10-methylacridine,<sup>17b</sup> which was proven to be the adduct of the 9-phenyl acridinium salt formed with an excess of MeOH (Figure S7 in Supporting Information). Similar trends were also observed in terms of chemical shift changes in the presence of  $\text{AcO}^-$ .

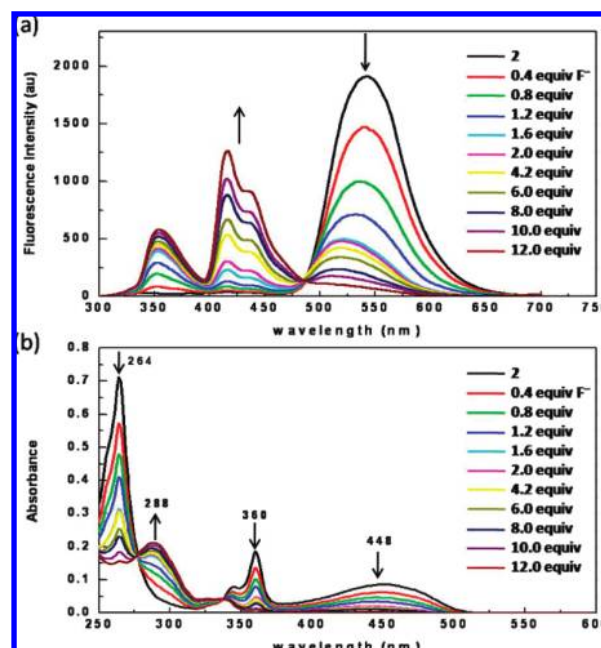


**Figure 2.** (a) Overlaid fluorescence spectra of **2** ( $10\ \mu\text{M}$  in  $\text{CH}_2\text{Cl}_2$ ) excited at 278 nm (the isosbestic point) and (b) the corresponding overlaid absorption spectra upon the addition of increasing amounts of  $\text{F}^-$ .

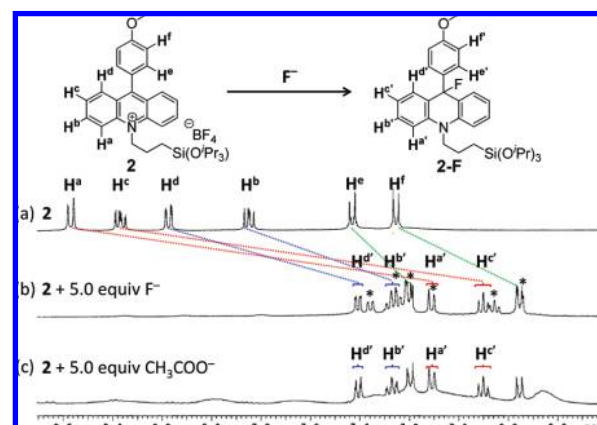


**Figure 3.** (a) Partial  $^1\text{H}$  NMR spectra (400 MHz, 5 mM, dichloromethane- $d_2$ , 25 °C) of **2** in the presence of 5 equiv of (b)  $\text{F}^-$  and (c)  $\text{CH}_3\text{COO}^-$ .

Notably, a byproduct (as denoted by the asterisks in Figure 3b) resulting from the strong Si–F interactions was formed upon the addition of 5 equiv of  $\text{F}^-$  to probe **2**.

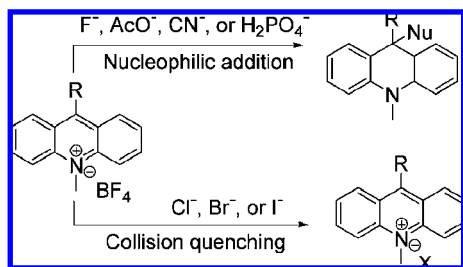
The results of photospectroscopy and  $^1\text{H}$  NMR studies clearly showed that the sensing mechanism was based on nucleophilic addition in the case of  $\text{F}^-$ ,  $\text{AcO}^-$ ,  $\text{CN}^-$ , and  $\text{H}_2\text{PO}_4^-$  and on collision quenching in the case of  $\text{Cl}^-$ ,  $\text{Br}^-$ , and  $\text{I}^-$ . The unequivocal sensing mechanisms for halides and for  $\text{F}^-$ ,  $\text{AcO}^-$ ,  $\text{CN}^-$ , and  $\text{H}_2\text{PO}_4^-$  are summarized in Scheme 3.

Exactly how the anion selectivities can be modulated through controlling steric congestion around the reactive site is further demonstrated by using probes **3** and **4**, having one

(23) Jones, G., II; Farahat, M. S.; Greenfield, S. R.; Gosztola, D. J.; Wasielewski, M. R. *Chem. Phys. Lett.* **1994**, 229, 40–46.



**Scheme 3.** Mechanisms of Anion-Dependent Sensing by Acridinium-Based Fluorescent Probes



or two methoxy groups enshrouding the C9 position of the acridinium. Additionally, the relationship between anion reactivity and steric congestion at the reactive site was further elucidated by using  $\text{F}^-$  (1.33 Å in diameter),<sup>24</sup>  $\text{AcO}^-$  (1.59 Å, triangular in shape),<sup>25</sup> and  $\text{H}_2\text{PO}_4^-$  (>2.0 Å, tetrahedral in shape),<sup>26</sup> which are in various sizes and proven to undergo the nucleophilic addition to probe **2**.<sup>27</sup>

As compared to probe **2**, a small blue shift (ca. 18 nm) is observed in the absorption maxima of **3** and **4**, indicating that the sterics diminish the co-planarity of the *ortho*-substituted phenyl ring and acridinium moiety. Upon treatment with 2 equiv of  $\text{F}^-$ , the absorption bands at 263, 360, and 430 nm in the spectrum of **3** disappeared entirely; however, no significant change is observed in the absorption spectrum of **4** (Figures S8 and S9 in Supporting Information). The sterics of two methoxy groups in probe **4** indeed effectively influences the nucleophilic addition trajectory, rendering a situation in which even small anions such as  $\text{F}^-$  cannot gain access to the reactive site. When larger anions,  $\text{AcO}^-$  and  $\text{H}_2\text{PO}_4^-$ , were used to react with **3**, only 40% conversion was observed for  $\text{AcO}^-$  and 12% for  $\text{H}_2\text{PO}_4^-$  within 2 h (Figure S8 in Supporting Information). Despite extending the reaction time to 5 h, probe **3** still cannot react with these two anions effectively. Comparing probes **1** and **2** reveals that **1** with no steric hindrance around the C9 position of acridinium can be easily attacked by anions of various sizes with 100% conversion within an hour; probe **2** having a 4'-methoxyphenyl group on the acridinium reacted with  $\text{F}^-$  and  $\text{AcO}^-$  readily and  $\text{H}_2\text{PO}_4^-$  partially (46% conversion) within 2 h.

The observed results could be rationalized in terms of the steric effect of the probes and strength of anion nucleophilicity, which are two dominant factors that govern the reactivity of nucleophilic addition. One may argue that the observed anion selectivity might result from varying degrees of solvation effects on anion nucleophilicity. Since our experiments were conducted in polar aprotic ( $\text{CH}_3\text{CN}$ ) and relatively nonpolar ( $\text{CH}_2\text{Cl}_2$ ) solvents, solvation effects on

the anions can be neglected. Thus, the size of monovalent anion becomes a decisive factor in the reactivity: the smaller the size of the anion, the stronger is the nucleophile.

Regeneration of the acridinium salt via treating either  $\text{NaBF}_4$  or an acid was demonstrated by monitoring UV-vis, fluorescence, and  $^1\text{H}$  NMR change of probe **1** (Figure 4). After excess  $\text{NaBF}_4$  was added, the absorption peaks corresponding to the acridinium salt reappeared, and the color of solution returned to pale yellow, as well as the blue-green fluorescence restored (Figure 4a).  $^1\text{H}$  NMR studies, as shown in Figure 4b, depicted the reformation of acridinium after adding 20% DCl, thereby providing conclusive evidence of the reversible process at the molecular level.

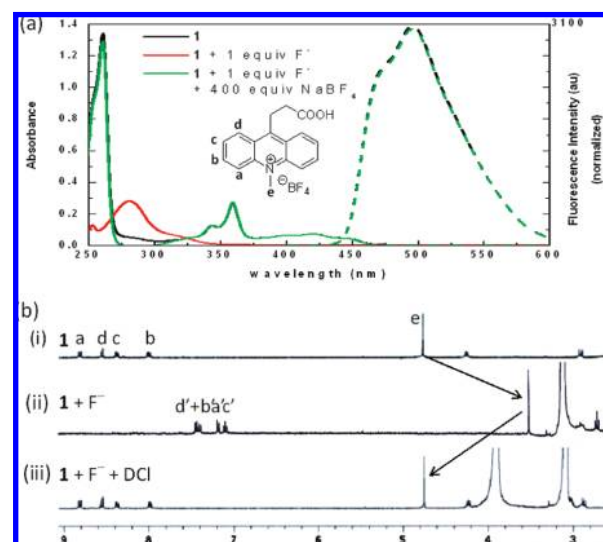


**Figure 4.** (a) Absorption (solid black line) and emission (dashed line) spectra of **1** (black, 10  $\mu\text{M}$  in  $\text{CH}_3\text{CN}$ ), **1** +  $\text{F}^-$  (red) and **1** +  $\text{F}^-$  + excess competitor  $\text{NaBF}_4$  (green). (b) Partial  $^1\text{H}$  NMR spectra (400 MHz, 10 mM, acetonitrile- $d_3$ , 25  $^\circ\text{C}$ ) of (i) **1**; (ii) **1** +  $\text{F}^-$ ; and (iii) **1** +  $\text{F}^-$  + 20% DCl.

In summary, our studies have established unequivocally the sensing mechanisms of acridinium-based fluorescent probes for halides such as  $\text{Cl}^-$ ,  $\text{Br}^-$ , and  $\text{I}^-$  and nucleophilic anions such as  $\text{F}^-$ ,  $\text{AcO}^-$ , and  $\text{H}_2\text{PO}_4^-$ . Further insights are also provided into how to steric congestion around the reactive site allows us to alter the anion selectivity in acridinium-based probes via nucleophilic addition. Most importantly, the sensory actions based on this molecular scaffold are reversible.

**Acknowledgment.** The authors thank the National Science Council of the Republic of China, Taiwan, for financial support.

**Supporting Information Available:** Selected synthetic procedures, structural characterization, and photospectroscopic data of acridinium salts. This material is available free of charge via the Internet at <http://pubs.acs.org>.

OL901935G

(24) Zhang, B.-G.; Cai, P.; Duan, C.-Y.; Miao, R.; Zhu, L.-G.; Niitsu, T.; Inoue, H. *Chem. Commun.* **2004**, 2206–2207.

(25) Zimmerman, G. H.; Wood, R. H. *J. Solution Chem.* **2002**, *31*, 995–1017.

(26) (a) Polanams, J.; Ray, A. D.; Watt, R. K. *Inorg. Chem.* **2005**, *44*, 3203–3209. (b) Kandori, K.; Uchida, S.; Kataoka, S.; Ishikawa, T. *J. Mater. Sci.* **1992**, *27*, 719–728.

(27) Powerful nucleophiles such as  $\text{CN}^-$  (log scale of its nucleophilicity is 5.1) would level the steric effects. Thus, only anions with moderate nucleophilicity were used in this study.